Atmospheric Environment 45 (2011) 6225–6232

Contents lists available at SciVerse ScienceDirect

Atmospheric Environment

journal homepage: www.elsevier.com/locate/atmosenv

Satellite-based estimates of ground-level fine particulate matter during extreme events: A case study of the Moscow fires in 2010

Aaron van Donkelaar [a,*], Randall V. Martin [a,b], Robert C. Levy [c], Arlindo M. da Silva [d], Michal Krzyzanowski [e], Natalia E. Chubarova [f], Eugenia Semutnikova [g], Aaron J. Cohen [h]

[a] Department of Physics and Atmospheric Science, Dalhousie University, 6300 Coburg Road, Halifax, NS B3H 3J5, Canada
[b] Harvard-Smithsonian Center for Astrophysics, Cambridge, MA, USA
[c] NASA Goddard Space Flight Center, Greenbelt, MD, USA
[d] Global Modeling and Assimilation Office, NASA Goddard Space Flight Center, Greenbelt, MD, USA
[e] European Centre for Environment and Health, WHO Regional Office for Europe, Bonn, Germany
[f] Geography Department, Moscow State University, Moscow, Russia
[g] State Environmental Organization, Mosecomonitoring, Moscow, Russia
[h] Health Effects Institute, Boston, MA, USA

ARTICLE INFO

Article history:
Received 20 April 2011
Received in revised form
20 July 2011
Accepted 25 July 2011

Keywords:
MODIS
$PM_{2.5}$
Moscow wildfires
Aerosol optical depth

ABSTRACT

We estimate fine particulate matter ($PM_{2.5}$) concentrations daily using MODIS satellite observations of aerosol optical depth (AOD) for a major biomass burning event around Moscow during summer 2010. Evaluation of MODIS AOD with the Moscow AERONET site supports a MODIS-AOD error estimate of $\pm(0.05 + 0.2 \times \mathrm{AOD})$ for this event. However, since the smoke was often thick (AOD > 4.0) and spatially variable, the standard MODIS algorithm incorrectly identifies some aerosol as cloud. We test relaxed cloud screening criteria that increase MODIS coverage by 21% and find excellent agreement with coincident operational retrievals ($r^2 = 0.994$, slope = 1.01) with no evidence of false aerosol detection. We relate the resultant MODIS AOD to $PM_{2.5}$ using aerosol vertical profiles from the GEOS-Chem chemical transport model. Our estimates are in good agreement with $PM_{2.5}$ values estimated from in-situ PM_{10} ($r^2 = 0.85$, slope = 1.06), and we find that the relationship between AOD and $PM_{2.5}$ is insensitive to uncertainties in biomass burning emissions. The satellite-derived and in-situ values both indicate that peak daily mean concentrations of approximately 600 $\mu g\, m^{-3}$ occurred on August 7, 2010 in the Moscow region of the Russian Federation. We estimate that exposure to air pollution from the Moscow wildfires may have caused hundreds of excess deaths.

1. Introduction

Extensive fires occurred in the Moscow region of the Russian Federation starting in late July 2010. No estimates of the health impacts of the Moscow fires have been published to date, but it is reasonable to assume that these extreme, short-lived excursions in ambient air pollution resulted in serious adverse health effects. Large short-term increases in air pollution, or air pollution episodes, in the mid-twentieth century were associated with rapid and pronounced increases in mortality from respiratory and cardiovascular disease (Anderson, 1999). More recent evidence links massive biomass burning from agricultural burning and forest fires to adverse health effects that range from minor irritation of the eyes and respiratory system to increased rates of hospital admissions for respiratory disease and mortality (Naeher et al., 2007). However, ground-level monitors are often sparse or unavailable in regions affected by fires. Additional observations are needed to assess pollutant concentrations and possible health impacts.

Satellite remote sensing of atmospheric aerosol provides a rich data source about particulate matter concentrations and is increasingly being used for health assessment studies during biomass burning events (e.g. Henderson et al., 2011; Rappold et al., 2011). Algorithmic developments continue to improve the accuracy with which ground-levelfine aerosol mass ($PM_{2.5}$) can be estimated from satellite remote sensing. These estimates use aerosol optical depth (AOD), a measure of the total extinction by aerosol of light passing through the atmospheric column, to estimate $PM_{2.5}$ through physical,

* Corresponding author. Tel.: +1 902 494 1820.
E-mail addresses: aaron.van.Donkelaar@dal.ca (A. van Donkelaar), randall.martin@dal.ca (R.V. Martin), robert.c.levy@nasa.gov (R.C. Levy), arlindo.m.dasilva@nasa.gov (A.M. da Silva), mkr@ecehbonn.euro.who.int (M. Krzyzanowski), chubarova@imp.kiae.ru (N.E. Chubarova), info@mosecom.ru (E. Semutnikova), acohen@healtheffects.org (A.J. Cohen).

1352-2310/$ – see front matter © 2011 Elsevier Ltd. All rights reserved.
doi:10.1016/j.atmosenv.2011.07.068

statistical or hybrid relationships developed from ground-level $PM_{2.5}$ measurements (e.g. Gupta et al., 2006; Koelemeijer et al., 2006; Liu et al., 2007, 2005; Wang and Christopher, 2003). Local observations of $PM_{2.5}$, vertical structure and relative humidity have all been used to improve the accuracy of remotely sensed $PM_{2.5}$ (e.g. Di Nicolantonio et al., 2009; Engel-Cox et al., 2006; Schaap et al., 2008).

Chemical transport models, which calculate the four-dimensional distribution of atmospheric aerosol mass, can accurately relate AOD to ground-level $PM_{2.5}$, allowing estimates in locations without nearby ground-based observations (Drury et al., 2010; Liu et al., 2004; van Donkelaar et al., 2010, 2006; Wang et al., 2010). Here we apply this approach to the Moscow wildfires to test its performance during major short-term pollution events.

The next section describes our approach to estimate $PM_{2.5}$ by interpreting AOD retrievals from the Moderate Resolution Imaging Spectroradiometer (MODIS) using the GEOS-Chem chemical transport model. Results are given and compared with in-situ $PM_{2.5}$ estimates. Developments to the operational MODIS aerosol retrieval algorithm for extreme events and the sensitivity of the AOD to $PM_{2.5}$ relationship to local emissions are also discussed. The subsequent section extends previous studies of extreme $PM_{2.5}$ events to estimate the excess mortality in Moscow during this period.

2. Retrieval of aerosol optical depth during extreme events

We first examine the MODIS AOD retrieval during the Moscow fires. The MODIS instrument obtains near daily global coverage at 32 spectral bands at a resolution of 250–1000 m, depending on the channel. Two MODIS instruments are currently in operation. The first, onboard the NASA Terra satellite, was launched in 1999 with a 10:30 a.m. local equatorial overpass time. The second, onboard the NASA Aqua satellite, was launched in 2002 with a 1:30 p.m. local equatorial overpass time. The wide spectral range and swath width of these versatile instruments has allowed for an AOD retrieval (Levy et al., 2007) at 10 km × 10 km with good accuracy $\pm(0.05 + 0.15 \times \mathrm{AOD})$; Remer et al., 2008) that has proven valuable for both daily and long-term observations of aerosol. However, most previous evaluation of MODIS AOD has been for typical values.

We turn to Aerosol Robotic Network (AERONET; Holben et al., 1998) sun photometer measurements to test whether this accuracy holds for the high aerosol loading that occurred during the fires. A complication is that the sun photometer relies on direct solar radiation. At extremely high AOD (above approximately 4–5) only limited direct radiation reaches the instrument and AERONET measurements are often not possible (Tom Eck, personal communication, 2011). The highest measured AERONET level 2.0 value during the Moscow wildfires is 4.3. We thus restrict MODIS AOD to values below 4.3 during comparison, to be consistent with AERONET. The top panel of Fig. 1 compares daily MODIS AOD in the Moscow region with AOD from the Moscow AERONET station for AOD above 0.5 between July 26 and August 20, 2010. The MODIS retrieval is consistent with AERONET under these conditions (slope = 0.90; bias = 0.11; $r^2 = 0.72$; $n = 14$). We find that 8 of 14 points lie within $\pm(0.05 + 0.2 \times \mathrm{AOD})$, which is slightly higher than typical operational error estimates.

Detection and removal of clouds is an important part of the MODIS AOD retrieval, since AOD is not retrieved in the presence of cloud. The operational MODIS AOD product (MOD04 and MYD04) detects cloud-contaminated pixels at 500 m resolution using spatial variability and brightness at 0.47 μm and 1.38 μm (Remer et al., 2006). The center pixel of each 3 × 3 group of pixels is designated as cloudy if the standard deviation of the group's reflectance is >0.0025 at 0.47 μm or >0.025 at 1.38 μm. These criteria use the small-scale variability that is typical of clouds but abnormal in aerosol to identify cloudy pixels. The 1.38 μm channel is sensitive to cirrus clouds. Any pixel with a 0.47 μm reflectance >0.4 is also considered cloudy, since clouds are highly reflective at this wavelength. Pixels on the granule perimeter are masked according to their neighbor. In addition to cloud masking, any retrieved AOD greater than 5.0 is removed. These criteria are typically effective, yet during extreme events aerosol plumes may be mistaken for cloud or AOD may exceed 5.0.

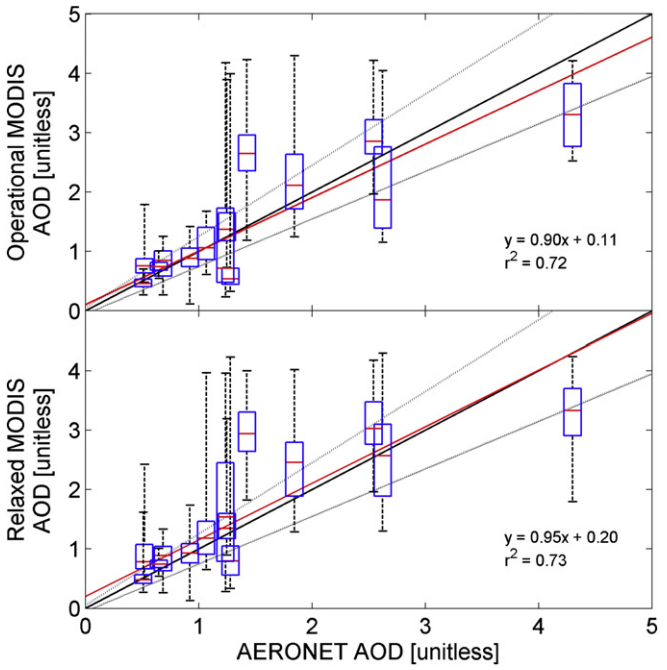

Fig. 1. Comparison of AERONET and MODIS for enhanced AOD above 0.5 in the Moscow region between July 26–August 20, 2011. The upper panel shows the operational MODIS retrieval and the lower panel shows the MODIS retrieval with the relaxed cloud criteria. Red horizontal lines and blue boxes denote the medians and 25th–75th percentiles of MODIS AOD. The line of best fit is shown in red. Unity and $\pm(0.05 + 0.2 \times \mathrm{AOD})$ are shown as the solid and dotted black lines, respectively. All AOD values are limited to a maximum of 4.3 for consistency with AERONET values. All AOD are at 550 nm, with AERONET adjusted from 500 nm to 550 nm via the local angstrom exponent. Vertical bars denote the full range of MODIS values (For interpretation of the references to colour in this figure legend, the reader is referred to the web version of this article.).

The left panel of Fig. 2 shows a MODIS Terra RGB image from August 8, 2010 at 08:50 UTC. Dense forest fire smoke is visible as gray plumes over the Moscow region, in contrast with white clouds to the east and west. The operational MODIS AOD retrieval, shown in the middle panel, correctly removes pixels affected by cloud, but also removes much of the dense aerosol plume over Moscow.

We explore the effects of relaxing the cloud screening criteria to increase coverage of the AOD retrieval. The maximum allowed spatial variability at 0.47 μm is doubled to 0.005. Additionally, if this 0.47 μm threshold is exceeded, but the 2.1 μm variability is <0.025, a pixel is classified as aerosol. The latter criterion reflects the transparency of fine aerosol at long wavelengths relative to cloud or dust (Kaufman et al., 1997). Finally, we increase the maximum allowed AOD to 10.0 to allow for dense smoke.

The result of this relaxed cloud filter is shown in the right panel of Fig. 2. A pronounced aerosol plume becomes evident, but the cloud screening on the edge of the region remains intact. The coverage is increased over Moscow although some peaks of the plume remain unretrieved. The relaxed filter has significant agreement ($r^2 = 0.995$) with the operational product and negligible bias (slope = 1.017), yet retains an additional 2275 10 km × 10 km

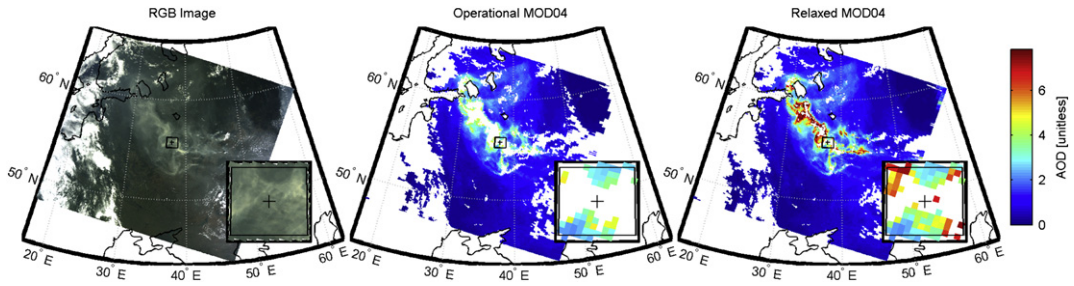

Fig. 2. The MODIS Terra granule from August 8, 2010 08:50 UTC. From left to right, the RGB image, the operational 550 nm AOD retrieval and the relaxed criteria 550 nm AOD retrieval are shown. The black crosshair and box identify Moscow and the Moscow Region, respectively, and are enlarged within the lower right subplot of each panel.

pixels for a range of AOD levels. We reprocess MODIS Aqua and Terra granules using our relaxed criteria between 30°E–60°E and 50°N–65°N between July 26, 2010 to August 20, 2010.

Fig. 3 compares MODIS AOD retrieved using the operational and relaxed criteria. On average the relaxed criteria retained an additional 21.3% of pixels from the 238 granules processed, generally with an increasing amount of additional coverage at higher AOD. The agreement between the relaxed and operational retrievals is high ($r^2 = 0.994$; slope = 1.010; offset = 0.004), and both show similar distributions. While there is no clear quantitative approach to assess the level of cloud contamination within the relaxed product, visual inspection of these granules suggests the large majority of additional pixels represent aerosol.

We again turn to AERONET in an attempt to further evaluate the performance of the relaxed cloud screening product. The bottom panel of Fig. 1 compares AERONET AOD with daily relaxed MODIS retrievals in the Moscow region at 550 nm. We again limit the maximum MODIS AOD to 4.3 for this comparison and compare only AERONET AOD above 0.5. The relaxed cloud criteria provides similar agreement (slope = 0.95; bias = 0.20; $r^2 = 0.73$; 7 of 14 points within $\pm(0.05 + 0.2 \times \mathrm{AOD})$) as the operational product, suggesting cloud contamination has not significantly impacted the results. The comparison retains some ambiguity due to the exact cutoff in AERONET measurements for high values. The balance of evidence from the visual evaluation and comparison, however, warrants applying the relaxed cloud screening for the local event.

3. Estimating ground-level aerosol pollution from satellite observations

We use the GEOS-Chem chemical transport model (Bey et al., 2001; v8-03-01; http://geos-chem.org) to relate AOD to ground-level $PM_{2.5}$ concentrations. The GEOS-Chem model solves for the temporal and spatial evolution of aerosol and trace gases using meteorological data sets, emission inventories, and equations that represent the physics and chemistry of atmospheric composition. The GEOS-Chem aerosol simulation includes the sulphate–ammonium–nitrate–water system (Park et al., 2004), primary carbonaceous aerosols (Park et al., 2003), secondary organic aerosols (Henze et al., 2008), sea-salt (Alexander et al., 2005), and mineral dust (Fairlie et al., 2007). Gas–aerosol equilibrium is computed using ISORROPIA II (Pye et al., 2009). The aerosol and oxidant simulations are coupled through formation of sulphate and nitrate (Park et al., 2004), heterogeneous chemistry (Evans and Jacob, 2005; Jacob, 2000; Thornton et al., 2008), and aerosol effects on photolysis rates (Lee et al., 2009; Martin et al., 2003).

This GEOS-Chem simulation uses assimilated meteorology from the Goddard Earth Observing System (GEOS-5), degraded to $2^\circ \times 2.5^\circ$ horizontal resolution and 47 vertical levels. Global anthropogenic emissions are based upon EDGAR 3.2FT2000 (Olivier et al., 2002), and scaled to 2006 following the approach of van Donkelaar et al. (2008). Global anthropogenic emissions are overwritten in areas with regional inventories, such as the European Monitoring and Evaluation Programme (EMEP; http://www.emep.int/) over Europe. We use daily Quick Fire Emissions Database version 2.1 (QFED v2.1) biomass burning emissions of organic carbon, black carbon and SO_2. QFED v2.1relates emissions to MODIS retrieved Fire Radiative Power via biome-specific calibration constants and observed area following Kaiser et al. (2009). QFED 2.1 is calibrated to produce global average biomass emissions consistent with the Global Fire Emission Database version 2(GFED v2; van der Werf et al., 2006). Biomass burning emissions in GEOS-Chem are released into the lowest model level and mix rapidly in the planetary boundary layer. Smoldering fires, such as from peat, likely emit predominantly into the planetary boundary layer as represented by this simple scheme (Turquety et al., 2007).

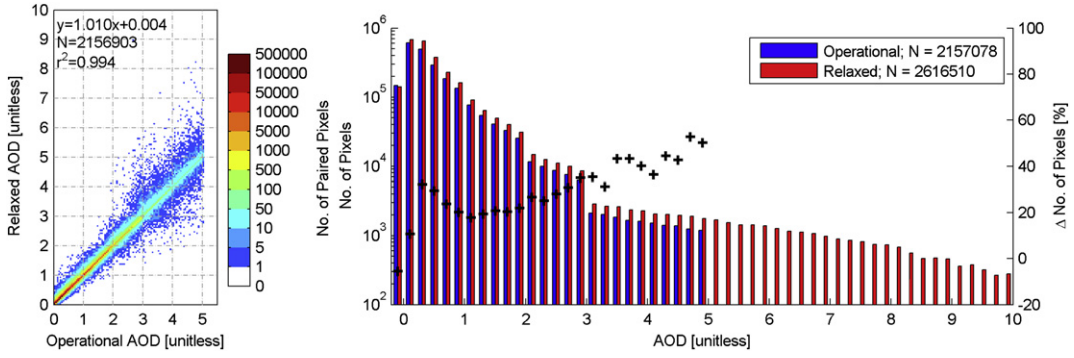

Fig. 3. Comparison of 550 nm MODIS AOD from the operational and relaxed criteria. Both panels compare all pixels from the 238 reprocessed granules. The right panel plots both the total number of retrievals (bars) and the percent change in number of AOD retrievals (pluses).

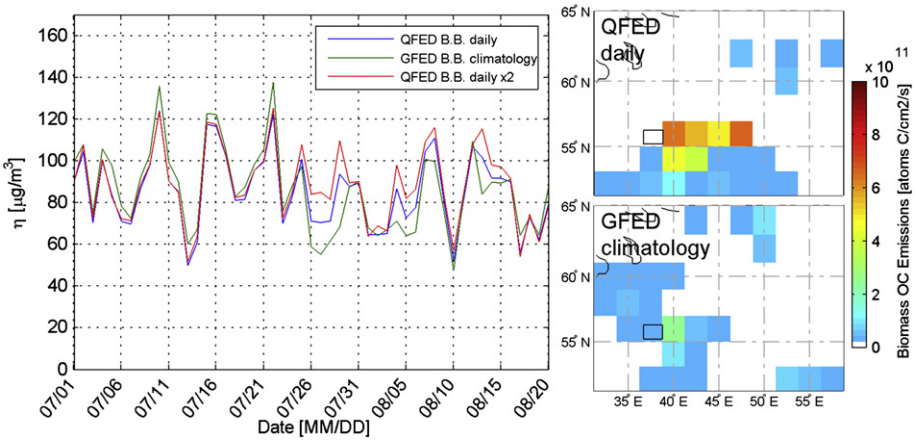

Fig. 4. Effect of emissions on the AOD to $PM_{2.5}$ relationship (η). The left panel shows simulated η using daily QFED, GFED climatological and doubled daily QFED biomass burning emissions. The right panels show daily average organic carbon (OC) emissions from July 22, 2010 to August 20, 2010. The black box identifies the Moscow region.

Following van Donkelaar et al. (2010), we estimate $PM_{2.5}$ as

$$PM_{2.5} = \eta \times AOD \quad (1)$$

where η is determined from the ratio of simulated $PM_{2.5}$ to simulated AOD at satellite overpass. η is a function of aerosol size, aerosol type, relative humidity, and the vertical structure of aerosol extinction.

Of concern for our application is the sensitivity of η to error in aerosol sources during this unusual event. For example, Yurganov et al. (2011) found evidence that space-based CO emissions during the Moscow wildfires were underestimated by a factor of 2–3. We test the robustness of η to this uncertainty through two sensitivity tests. First, we compare values of η resultant from doubling QFED 2.1 emissions. Second, we compare values of η calculated using climatological monthly average biomass burning emissions from a different inventory, GFED2. GFED2 v2 calculates biomass burning emissions as a function of time varying precipitation, temperature, solar radiation and fractional-absorbed photosynthetically active radiation (Giglio et al., 2006).

The right panels of Fig. 4 show the organic carbon emissions from monthly mean 1997–2008 GFED v2 emissions and the average QFED v2.1 emissions for July 22–August 20, 2010. Both inventories have peak mean organic carbon emissions east of Moscow, but the period-specific QFED v2.1 emissions have much higher emissions and broader sources extending further east.

The left panel of Fig. 4 shows the time series of η from July 1, 2010 to August 20, 2010. Values of η show little difference (typically $< 10\%$) whether using daily (QFED), climatological (GFED), or daily doubled (QFED $\times$ 2) biomass burning emissions, despite large changes in emissions (right panels). The average difference in η between all three emission scenarios is 15% during the peak influence of the fires (August 1–10, 2010), giving an indication of the uncertainty in this parameter. The time series is influenced by a variety of processes such as wind direction and planetary boundary layer height that affect the vertical profile of the aerosol extinction. We take an additional 15% error to represent uncertainties these other parameters which will impact the accuracy of η. Adding these uncertainties in quadrature with the observed uncertainty in AOD yields a combined uncertainty of 30% in the satellite-derived $PM_{2.5}$ estimates during the fires.

Fig. 5 shows mean satellite-derived $PM_{2.5}$ concentrations in the Moscow region for the period from July 7 to 21, 2010, leading up to the fire event. Mean satellite-derived $PM_{2.5}$ concentrations range from 13.1–35.7 $\mu g\, m^{-3}$, and have enhancements in the urban core. We evaluate these concentrations with in-situ measurements. Two in-situ Tapered Element Oscillating Microbalance (TEOM) $PM_{2.5}$ monitors were operational in Moscow during this period, but only PM_{10}measurements were available outside the city center. We estimate $PM_{2.5}$ concentrations from the PM_{10} measurements using the mean measured aerosol fine fraction ($PM_{2.5}/PM_{10}$) of 66.8%

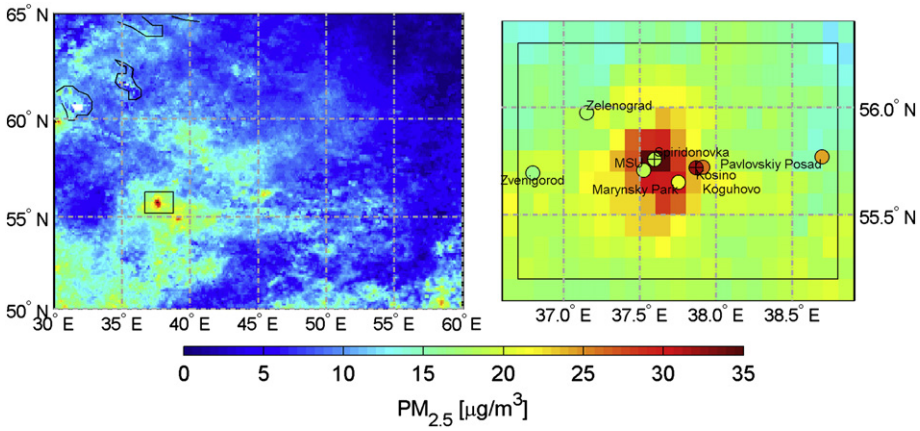

Fig. 5. Satellite-derived mean $PM_{2.5}$ for July 7–21, 2010. The Moscow region is shown by the black box and enlarged in the right-hand panel. Filled circles give in-situ values, with cross-haired locations denoting direct $PM_{2.5}$ measurements with others estimated from in-situ PM_{10}. Table 1 provides details of each station.

Table 1
Aerosol monitoring stations in the Moscow region, Russian Federation.

Station	Type	Class	Coordinates	In-situ $PM_{2.5}$[a]			
				July 7–21, 2010[b]		August 3–10, 2010[c]	
				Mean (range) $\mu g\,m^{-3}$	No. of obs.	Mean (range) $\mu g\,m^{-3}$	No. of obs.
Marymsky Park	PM_{10}	Urban	55°39′8.45″N, 37°45′4.92″E	21.0 (12.7–34.1)	15	262 (73.6–608)	8
Zelenograd	PM_{10}	Suburban	55°58′38.69″N, 37°09′1.49″E	18.0 (10.7–27.4)	15	275 (109–518)	8
MSU	PM_{10}	Suburban	55°42′26.45″N, 37°31′20.60″E	18.7 (18.7–18.7)	1	264 (51.2–611)	8
Kosino	$PM_{2.5}$, PM_{10}	Urban	55°43′13.40″N, 37°52′2.96″E	32.1 (21.0–41.0)	8	333 (114–725)	8
Spiridonovka	$PM_{2.5}$, PM_{10}	Urban	55°45′33.55″N, 37°35′43.84″E	18.6 (13.0–25.0)	8	270 (107–382)	3
Pavlovsky Posad	PM_{10}	Rural background	55°46′16.45″N, 38°41′34.02″E	24.3 (12.7–42.8)	10	236 (55.2–564)	8
Zvenigorod	PM_{10}	Rural background	55°41′49.44″N, 36°47′44.14″E	16.7 (15.4–17.4)	4	223 (84.0–447)	5
Kozhuhovo	PM_{10}	Suburban	55°43′21.66″N; 37°54′37.69″E	26.1 (14.7–39.4)	13	326 (114–673)	8

[a] $PM_{2.5}$ is estimated from PM_{10} with the exception of Kosino and Spirionovka for July 7–21, 2010.
[b] A constant fine fraction of 66.8% is used, based upon coincident $PM_{2.5}$ and PM_{10} measurements at Kosino and Spirionovka between July 7–21, 2010.
[c] A constant fine fraction of 80% is used during the biomass burning event (Alves et al., 2010; Martin et al., 2010).

during this time using PM_{10} measurements coincident with the two $PM_{2.5}$ monitors. Similar to our satellite-derived estimates, daily mean in-situ $PM_{2.5}$ (Table 1) range from 16.7–32.1 $\mu g\,m^{-3}$ during this time. Differences between in-situ and satellite-derived $PM_{2.5}$ spatial patterns possibly reflect differences in spatial representativeness between these metrics or daily/spatial deviations in the fine fraction applied to PM_{10}, as well as errors the in-situ and satellite-derived value themselves.

The two $PM_{2.5}$ TEOM monitors were not in operation during the wildfire event. We continue to estimate in-situ $PM_{2.5}$ from the PM_{10} monitors that did remain in operation throughout the event by applying the fine fraction of 80% inferred from measurements of other biomass burning events (Alves et al., 2010; Martin et al., 2010). Fig. 6 compares in-situ and satellite-derived $PM_{2.5}$ between July 14, 2010 and August 18, 2010. Both metrics show good agreement ($r^2 = 0.85$, slope = 1.06), with in-situ values in the range of satellite-derived $PM_{2.5}$. A peak value of approximately 600 $\mu g\,m^{-3}$ is given by both metrics on August 7, 2010. A sensitivity study in which $PM_{2.5}$ was derived using the operational MODIS AOD product reduced agreement with in-situ values due to filtration of aerosol by the operational cloud filter, and provides further evidence for using the relaxed cloud screening algorithm for this event.

Fig. 7 shows regional mean daily overpass $PM_{2.5}$ estimates from MODIS Aqua and Terra for August 3–10, 2010. Extremely high levels of $PM_{2.5}$ span hundreds of thousands of square kilometers. The largest plumes intercept Moscow on August 6–9, 2010.

4. Health impacts of the Moscow fires

Although direct estimates of health impacts of the Moscow fires are not currently available, some insight into the possible magnitude of the health impacts caused by the fires can come from considering the quantitative impacts that have been observed in time series studies associating the daily changes in population mortality with daily average concentration of particulate matter.

We estimate the increased relative risk of death (ΔRR_d) on a day with PM_{10} concentration C_d based on the relative risk estimate of RR (per 10 $\mu g\,m^{-3}$ PM_{10}) inferred from the meta-analysis of time-series studies according to the form

$$\Delta RR_d = (RR - 1)(C_d - C_r)/10 \quad (2)$$

where C_r is the reference concentration of PM_{10} (in the absence of the fires).

The excess mortality on day d was calculated as

$$\Delta M_d = M \cdot \Delta RR_d/(\Delta RR_d + 1) \quad (3)$$

where M is the expected number of deaths per day in the absence of fires.

The meta-analysis of European studies, conducted in 33 cities, indicated a 10 $\mu g\,m^{-3}$ increase in daily PM_{10} levels is associated with 0.6% (95% Confident Interval (CI) 0.4%–0.8%) increase in total daily number of deaths (WHO, 2005). Similar risks were estimated by studies conducted in Asia (Wong et al., 2008). Assuming

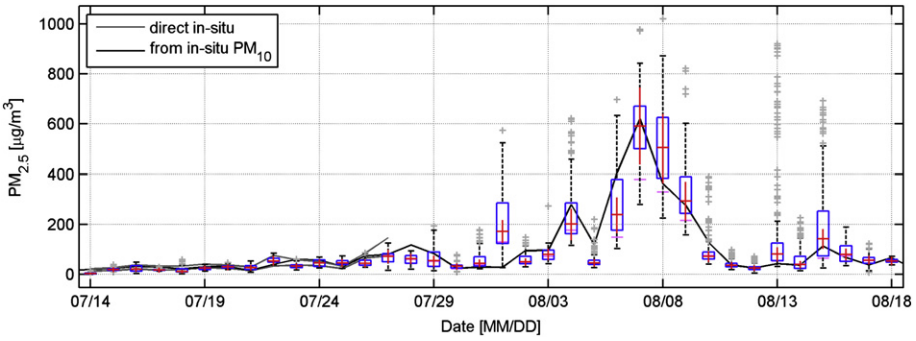

Fig. 6. Comparison of in-situ and satellite-derived $PM_{2.5}$ during the summer 2010 fire event. The box and whisker plot presents satellite-derived $PM_{2.5}$ within the boxed region of Figs. 1, 4, 5 and 7. Blue boxes surround the 25th and 75th percentiles of the satellite-derived $PM_{2.5}$. Medians and full ranges are given by the red horizontal lines and error bars, respectively. Uncertainty in median values are given by vertical red lines. Outliers are denoted by light grey pluses. All satellite-derived $PM_{2.5}$ values given here use the relaxed cloud screening product from MODIS, except for the magenta line which indicate median $PM_{2.5}$ derived from the operational MODIS AOD product. The black line denotes mean $PM_{2.5}$ estimated from in-situ PM_{10} monitors. Dark grey lines correspond to direct in-situ $PM_{2.5}$ measurements (For interpretation of the references to colour in this figure legend, the reader is referred to the web version of this article.).

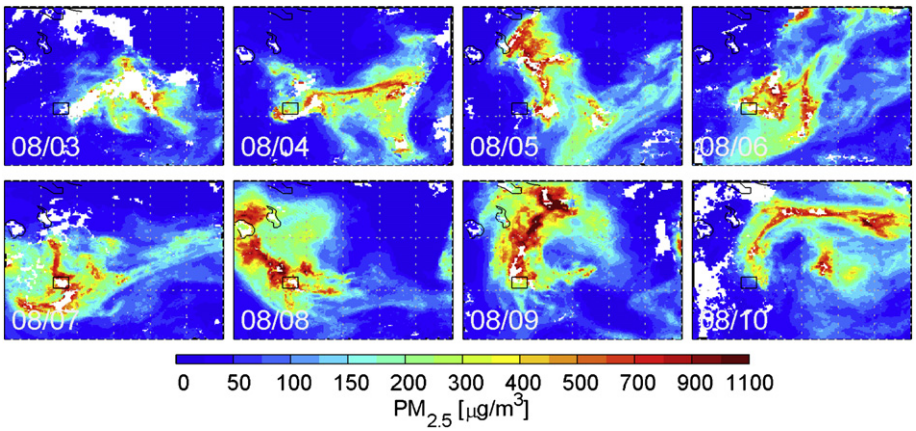

Fig. 7. Daily satellite-derived $PM_{2.5}$ from August 3–10, 2010. The black box identifies the Moscow region.

a similar association of daily mortality with PM_{10} levels in Moscow during the fires, enhancement of PM_{10} above the pre-fire level (27 μg m^{-3} for 7–21 July 2010), would lead to an average 14% (95% CI 9%–19%) increase in the risk of death during the fires (2–10 August). The CI is inferred from the combination of uncertainty in the $PM_{2.5}$ estimates and the uncertainty in the risk increase from PM. Fig. 8 shows the estimated number of daily deaths in Moscow due to smoke from the fires, given an approximate average daily number of deaths in Moscow of 400. This leads to an excess of about 434 deaths during this 9 day period (95% CI 263–583) (Fig. 8).

An additional source of information on the link between mortality and air pollution from forest fires is the analysis of impacts of fires that occurred in Indonesia in 1997 (Sastry, 2002). This study estimated an increase of all cause mortality in Kuala Lumpur, Malaysia, by 19% (Standard Error (SE) 10.9%) on high air pollution days ($PM_{10} > 210$ μg m^{-3}). Using this risk coefficient for days for high PM_{10} levels we can estimate an excess of about 64 deaths in each of the days in which PM_{10} exceeded 210 μg m^{-3} in Moscow, which suggests an excess of 320 deaths (95 CI: −48–575; $p < 0.10$) over the period of the fires. Sastry reported that the largest increase in mortality occurred among people 65–74 years of age (56%, SE 32.8%, Sastry, 2002, Table 4). Mortality increased by 21.8% (SE 8.6%), especially among infants and the 65–74 age group, on days of low visibility (<0.91 km) which is indicative of high air pollution from forest fires (Sastry, 2002, Table 8).

Together, these analyses suggest that hundreds of excess deaths occurred as a result of exposure to PM from the Moscow fires, a result consistent with expectations based on earlier episodes of very high air pollution. However, the true magnitude of the mortality impacts is difficult to quantify with precision. More definitive estimates of the health impacts of the fires would require a careful analysis of local data on morbidity and mortality for the relevant time periods, data that are currently unavailable. In addition, when high levels of biomass smoke are accompanied by extreme heat, as was the case in the Moscow fires, both air pollution and heat may cause serious adverse health effects, and the independent effect of increased exposure to air pollution may be difficult to quantify. Moreover, exposure to particulate air pollution and extreme heat may interact, resulting in effects that are more than additive (Qian et al., 2008). Both estimates given above assume a linear relation between short-term exposure to PM and the excess relative risk of mortality across a broad range of PM levels. However, Sastry (2002, Table 3) suggests that the relationship may be supra-linear at levels in excess of 200 μg m^{-3} PM_{10}, while others argue that there may be a marked decrease in the excess relative risk at very high levels of exposure (Pope et al., 2011). Furthermore, we estimate only the effects of exposure on the days of the episode. Health impacts over the longer term may be affected by both reduced mortality in the aftermath of the episode, so-called "harvesting" or "mortality displacement" (due to the depletion of frail or otherwise susceptible individuals), or by chronic effects caused by the extreme exposures (e.g. the long-term sequalae of acute myocardial infarctions brought on by the episode).

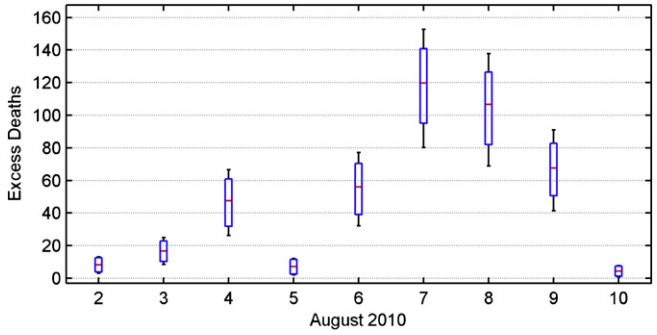

Fig. 8. Estimated number of daily deaths in Moscow due to smoke from the wildfires, August 2–10, 2010. Red line gives expected value. Blue box denotes range resulting from uncertainty in $PM_{2.5}$ estimates. Error bar denotes the overall 95% confidence interval (For interpretation of the references to colour in this figure legend, the reader is referred to the web version of this article.).

5. Conclusions

We estimated daily mean ground-level $PM_{2.5}$ concentrations from satellite observations during the major biomass burning event around Moscow in summer 2010. The GEOS-Chem model was used to relate aerosol optical depth (AOD) from the MODIS satellite instrument to ground-level $PM_{2.5}$ concentrations. We found that these satellite-derived estimates well represent ground-level $PM_{2.5}$ estimated from PM_{10} measurements ($r^2 = 0.85$, slope = 1.06). Peak daily mean satellite-derived $PM_{2.5}$ exceed 600 μg m^{-3} in the Moscow area on August7, 2010, with similar $PM_{2.5}$ values estimated from in-situ measurements of PM_{10}. $PM_{2.5}$ concentrations of several hundred μg m^{-3} were estimated to affect hundreds of thousands of square kilometers surrounding Moscow.

To contribute to these results, we presented a relaxed cloud screening criteria for the MODIS AOD retrieval algorithm that increases coverage during extreme aerosol events without apparent misclassification of clouds. The relaxed criteria allows

retrieval of an additional 21.3% of pixels during this period in the Moscow region. It has strong agreement with the operational retrieval algorithm for coincident pixels ($r^2 = 0.994$; slope = 1.010), with the recovered pixels spread across a range of AOD values. Evaluation of MODIS AOD from this product supports an AOD error estimate of $\pm(0.05 + 0.2 \times \mathrm{AOD})$ during this event. The relaxed screening algorithm improved the agreement of satellite-based $PM_{2.5}$ versus in-situ measurements during the fires. Further study is required to determine if these relaxed criteria perform well under more typical conditions.

We found that the relationship between AOD and $PM_{2.5}$ is robust to uncertainty in emissions. We evaluate the performance of MODIS AOD versus AERNET measurements during this event. The combined uncertainty in the satellite-based $PM_{2.5}$ concentrations was estimated as 30%. These results suggest that satellite observations can be used to monitor daily ground-level $PM_{2.5}$ during major events without direct calibration to in-situ $PM_{2.5}$.

Using concentration–response relationships from the scientific literature on the health effects of short-term exposure to PM, we estimated that exposure to air pollution from the Moscow wildfires may have caused hundreds of excess deaths.

6. Disclaimer

The views expressed in this paper are those of the authors and do not necessarily reflect the views of the Health Effects Institute or its sponsors.

Acknowledgements

This work was supported by the Natural Science and Engineering Research Council of Canada (NSERC) and the Killam Trust.

References

Alexander, B., Park, R.J., Jacob, D.J., Li, Q.B., Yantosca, R.M., Savarino, J., Lee, C.C.W., Thiemens, M.H., 2005. Sulfate formation in sea-salt aerosols: constraints from oxygen isotopes. Journal of Geophysical Research-Atmospheres 110.

Alves, C.A., Goncalves, C., Pio, C.A., Mirante, F., Caseiro, A., Tarelho, L., Freitas, M.C., Viegas, D.X., 2010. Smoke emissions from biomass burning in a Mediterranean shrub land. Atmospheric Environment 44, 3024–3033.

Anderson, H.R., 1999. Health effects of air pollution episodes. In: Samet, J., Koen, H., Maynard, R. (Eds.), Air Pollution and Health. Academic Press, London.

Bey, I., Jacob, D.J., Yantosca, R.M., Logan, J.A., Field, B.D., Fiore, A.M., Li, Q.B., Liu, H.G.Y., Mickley, L.J., Schultz, M.G., 2001. Global modeling of tropospheric chemistry with assimilated meteorology: model description and evaluation. Journal of Geophysical Research-Atmospheres 106, 23073–23095.

Di Nicolantonio, W., Cacciari, A., Tomasi, C., 2009. Particulate matter at surface: Northern Italy monitoring based on satellite remote sensing, meteorological fields, and in-situ sampling. IEEE Journal of Selected Topics in Applied Earth Observations and Remote Sensing 2, 284–292.

Drury, E., Jacob, D.J., Spurr, R.J.D., Wang, J., Shinozuka, Y., Anderson, B.E., Clarke, A.D., Dibb, J., McNaughton, C., Weber, R., 2010. Synthesis of satellite (MODIS), aircraft (ICARTT), and surface (IMPROVE, EPA-AQS, AERONET) aerosol observations over eastern North America to improve MODIS aerosol retrievals and constrain surface aerosol concentrations and sources. Journal of Geophysical Research-Atmospheres 115.

Engel-Cox, J.A., Hoff, R.M., Rogers, R., Dimmick, F., Rush, A.C., Szykman, J.J., Al-Saadi, J., Chu, D.A., Zell, E.R., 2006. Integrating lidar and satellite optical depth with ambient monitoring for 3-dimensional particulate characterization. Atmospheric Environment 40, 8056–8067.

Evans, M.J., Jacob, D.J., 2005. Impact of new laboratory studies of N2O5 hydrolysis on global model budgets of tropospheric nitrogen oxides, ozone, and OH. Geophysical Research Letters 32.

Fairlie, T.D., Jacob, D.J., Park, R.J., 2007. The impact of transpacific transport of mineral dust in the United States. Atmospheric Environment 41, 1251–1266.

Giglio, L., van der Werf, G.R., Randerson, J.T., Kasibhatla, P., 2006. Global estimation of burned area using MODIS active fire observations. Atmospheric Chemistry and Physics 6, 957–974.

Gupta, P., Christopher, S.A., Wang, J., Gehrig, R., Lee, Y., Kumar, N., 2006. Satellite remote sensing of particulate matter and air quality assessment over global cities. Atmospheric Environment 40, 5880–5892.

Henderson, S., Brauer, M., MacNab, Y.C., 2011. Three measures of forest fire smoke exposure and their associations with respiratory and cardiovascular health outcomes in a population-based cohort. Environmental Health Perspectives.

Henze, D.K., Seinfeld, J.H., Ng, N.L., Kroll, J.H., Fu, T.M., Jacob, D.J., Heald, C.L., 2008. Global modeling of secondary organic aerosol formation from aromatic hydrocarbons: high- vs. low-yield pathways. Atmospheric Chemistry and Physics 8, 2405–2421.

Holben, B.N., Eck, T.F., Slutsker, I., Tanre, D., Buis, J.P., Setzer, A., Vermote, E., Reagan, J.A., Kaufman, Y.J., Nakajima, T., Lavenu, F., Jankowiak, I., Smirnov, A., 1998. AERONET – a federated instrument network and data archive for aerosol characterization. Remote Sensing of Environment 66, 1–16.

Jacob, D.J., 2000. Heterogeneous chemistry and tropospheric ozone. Atmospheric Environment 34, 2131–2159.

Kaiser, J.W., Flemming, J., Schultz, M.G., Suttie, M., Wooster, M.J., 2009. The MACC global fire assimilation system: first emission products (GFASv0). ECMWF Tech. Memo No. 596.

Kaufman, Y.J., Tanre, D., Remer, L.A., Vermote, E.F., Chu, A., Holben, B.N., 1997. Operational remote sensing of tropospheric aerosol over land from EOS moderate resolution imaging spectroradiometer. Journal of Geophysical Research-Atmospheres 102, 17051–17067.

Koelemeijer, R.B.A., Homan, C.D., Matthijsen, J., 2006. Comparison of spatial and temporal variations of aerosol optical thickness and particulate matter over Europe. Atmospheric Environment 40, 5304–5315.

Lee, C., Martin, R.V., van Donkelaar, A., O'Byrne, G., Krotkov, N., Richter, A., Huey, L.G., Holloway, J.S., 2009. Retrieval of vertical columns of sulfur dioxide from SCIAMACHY and OMI: air mass factor algorithm development, validation, and error analysis. Journal of Geophysical Research-Atmospheres 114.

Levy, R.C., Remer, L.A., Mattoo, S., Vermote, E.F., Kaufman, Y.J., 2007. Second-generation operational algorithm: retrieval of aerosol properties over land from inversion of Moderate Resolution Imaging Spectroradiometer spectral reflectance. Journal of Geophysical Research-Atmospheres 112.

Liu, Y., Koutrakis, P., Kahn, R., 2007. Estimating fine particulate matter component concentrations and size distribution using satellite-retrieved fractional aerosol optical depth: Part 1-Method Development. Journal of Air & Waste Management Association 57, 1351–1359.

Liu, Y., Park, R.J., Jacob, D.J., Li, Q.B., Kilaru, V., Sarnat, J.A., 2004. Mapping annual mean ground-level PM2.5 concentrations using Multiangle Imaging Spectroradiometer aerosol optical thickness over the contiguous United States. Journal of Geophysical Research-Atmospheres 109.

Liu, Y., Sarnat, J.A., Kilaru, A., Jacob, D.J., Koutrakis, P., 2005. Estimating ground-level PM2.5 in the eastern United States using satellite remote sensing. Environmental Science & Technology 39, 3269–3278.

Martin, R.V., Jacob, D.J., Yantosca, R.M., Chin, M., Ginoux, P., 2003. Global and regional decreases in tropospheric oxidants from photochemical effects of aerosols. Journal of Geophysical Research-Atmospheres 108.

Martin, S.T., Andreae, M.O., Artaxo, P., Baumgardner, D., Chen, Q., Goldstein, A.H., Guenther, A., Heald, C.L., Mayol-Bracero, O.L., McMurry, P.H., Pauliquevis, T., Poschl, U., Prather, K.A., Roberts, G.C., Saleska, S.R., Dias, M.A.S., Spracklen, D.V., Swietlicki, E., Trebs, I., 2010. Sources and properties of Amazonian aerosol particles. Reviews of Geophysics 48.

Naeher, L.P., Brauer, M., Lipsett, M., Zelikoff, J.T., Simpson, C.D., Koenig, J.Q., Smith, K.R., 2007. Woodsmoke health effects: a review. Inhalation Toxicology 19, 67–106.

Olivier, J.G.J., Berdowski, J.J.M., Peters, J.A.H.W., Bakker, J., Visschedijk, A.J.H., Bloos, J.J., 2002. Applications of EDGAR including a description of EDGAR 3.2 reference database with trend data for 1970–1995. Document.

Park, R.J., Jacob, D.J., Chin, M., Martin, R.V., 2003. Sources of carbonaceous aerosols over the United States and implications for natural visibility. Journal of Geophysical Research-Atmospheres 108.

Park, R.J., Jacob, D.J., Field, B.D., Yantosca, R.M., Chin, M., 2004. Natural and transboundary pollution influences on sulfate-nitrate-ammonium aerosols in the United States: implications for policy. Journal of Geophysical Research-Atmospheres 109.

Pope, C.A.I., Brook, R.D., Burnett, R.T., Dockery, D.W., 2011. How is cardiovascular disease mortality risk affected by duration and intensity of fine particulate matter exposure? An integration of the epidemiologic evidence. Air Quality, Atmospheric and Health 4, 5–14.

Pye, H.O.T., Liao, H., Wu, S., Mickley, L.J., Jacob, D.J., Henze, D.K., Seinfeld, J.H., 2009. Effect of changes in climate and emissions on future sulfate–nitrate–ammonium aerosol levels in the United States. Journal of Geophysical Research 114 (D01205).

Qian, Z., He, Q., Lin, H.M., Kong, L., Bentley, C.M., Liu, W., Dinjin, Z., 2008. High temperatures enhanced acute mortality effects of ambient particle pollution in the "oven" city of Wuhan, China. Environmental Health Perspectives 116, 1172–1178.

Rappold, A.G., Stone, S.L., Cascio, W.E., Neas, L.M., Kilaru, V.J., Carraway, M.S., Szykman, J.J., Ising, A., Cleve, W.E., Meredith, J.T., Vaughan-Batten, H., Deyneka, L., Devlin, R.B., 2011. Peat bog wildfire smoke exposure in rural North Carolina is associated with cardio-pulmonary emergency department visits assessed through syndromic surveillance. Environmental Health Perspectives.

Remer, L.A., Kleidman, R.G., Levy, R.C., Kaufman, Y.J., Tanre, D., Mattoo, S., Martins, J.V., Ichoku, C., Koren, I., Yu, H.B., Holben, B.N., 2008. Global aerosol climatology from the MODIS satellite sensors. Journal of Geophysical Research-Atmospheres 113.

Remer, L.A., Tanré, D., Kaufman, Y.J., Levy, R.C., Mattoo, S., 2006. Algorithm for remote sensing of tropospheric aerosol from MODIS: collection 005. Algorithm Theoretical Basis Document.

Sastry, N., 2002. Forest fires, air pollution, and mortality in Southeast Asia. Demography 29, 1–23.
Schaap, M., Apituley, A., Timmermans, R.M.A., Koelemeijer, R.B.A., de Leeuw, G., 2008. Exploring the relation between aerosol optical depth and PM2.5 at Cabauw, the Netherlands. Atmospheric Chemistry and Physics Discussions 8, 17939–17986.
Thornton, J.A., Jaegle, L., McNeill, V.F., 2008. Assessing known pathways for HO2 loss in aqueous atmospheric aerosols: regional and global impacts on tropospheric oxidents. Journal of Geophysical Research-Atmospheres 113.
Turquety, S., Logan, J.A., Jacob, D.J., Hudman, R.C., Leung, F.Y., Heald, C.L., Yantosca, R.M., Wu, S., Emmons, L.K., Edwards, D.P., Sachse, G.W., 2007. Inventory of boreal fire emissions for North America in 2004: importance of peat burning and pyroconvective injection. Journal of Geophysical Research 112.
van der Werf, G.R., Randerson, J.T., Giglio, L., Collatz, G.J., Kasibhatla, P.S., Arellano, A.F.J., 2006. Interannual variability in global biomass burning emissions from 1997 to 2004. Atmospheric Chemistry and Physics 6, 3423–3441.
van Donkelaar, A., Martin, R.V., Brauer, M., Kahn, R.A., Levy, R.C., Verduzco, C., 2010. Global estimates of ambient fine particulate matter concentrations from satellite-based aerosol optical depth: development and application. Environmental Health Perspectives 118.
van Donkelaar, A., Martin, R.V., Leaitch, W.R., Macdonald, A.M., Walker, T.W., Streets, D.G., Zhang, Q., Dunlea, E.J., Jimenez, J.L., Dibb, J.E., Huey, L.G., Weber, R., Andreae, M.O., 2008. Analysis of aircraft and satellite measurements from the Intercontinental Chemical Transport Experiment (INTEX-B) to quantify long-range transport of East Asian sulfur to Canada. Atmospheric Chemistry and Physics 8, 2999–3014.
van Donkelaar, A., Martin, R.V., Park, R.J., 2006. Estimating ground-level PM2.5 using aerosol optical depth determined from satellite remote sensing. Journal of Geophysical Research-Atmospheres 111.
Wang, J., Christopher, S.A., 2003. Intercomparison between satellite-derived aerosol optical thickness and PM2.5 mass: Implications for air quality studies. Geophysical Research Letters 30.
Wang, J., Xu, X.G., Spurr, R., Wang, Y.X., Drury, E., 2010. Improved algorithm for MODIS satellite retrievals of aerosol optical thickness over land in dusty atmosphere: implications for air quality monitoring in China. Remote Sensing of Environment 114, 2575–2583.
WHO Regional Office for Europe, 2005. Air Quality Guidelines – Global Update 2005. Copenhagen, WHO Regional Office for Europe. http://www.euro.who.int/__data/assets/pdf_file/0005/78638/E90038.pdf.
Wong, C.M., Vichit-Vadakan, N., Kan, H., Qian, Z., Teams, P.P., 2008. Public Health and Air Pollution in Asia (PAPA): a multicity study of short-term effects of air pollution on mortality. Environmental Health Perspectives 116, 1195–1202.
Yurganov, L., Rakitin, V., Dzhola, A., August, T., Fokeeva, E., Gorchakov, G., Grechko, E., Hannon, S., Karpov, A., Ott, L., Semutnikova, E., Shumsky, R., Strow, L., 2011. Satellite- and ground-based CO total column observations over 2010 Russian fires: accuracy of top-down estimates based on thermal IR satellite data. Atmospheric Chemistry and Physics Discussions 11, 12207–12250.